Journal of Solid State Chemistry 184 (2011) 1858–1866

Contents lists available at ScienceDirect

Journal of Solid State Chemistry

journal homepage: www.elsevier.com/locate/jssc

Chloride substitution in sodium borohydride

Dorthe B. Ravnsbæk, Line H. Rude, Torben R. Jensen*

Center for Materials Crystallography (CMC), Interdisciplinary Nanoscience Center (iNANO), Department of Chemistry, Aarhus University, Langelandsgade 140, DK-8000 Århus C, Denmark

ARTICLE INFO

Article history:
Received 3 March 2011
Received in revised form
16 May 2011
Accepted 23 May 2011
Available online 30 May 2011

Keywords:
Hydrogen storage
Solid solutions
Anion substitution
X-ray diffraction
Solid state diffusion

ABSTRACT

The dissolution of sodium chloride and sodium borohydride into each other resulting in formation of solid solutions of composition $Na(BH_4)_{1-x}Cl_x$ is studied. The dissolution reaction is facilitated by two methods: ball milling or combination of ball milling and annealing at 300 °C for three days of $NaBH_4$–NaCl samples in molar ratios of 0.5:0.5 and 0.75:0.25. The degree of dissolution is studied by Rietveld refinement of synchrotron radiation powder X-ray diffraction (SR-PXD) data. The results show that dissolution of 10 mol% NaCl into $NaBH_4$, forming $Na(BH_4)_{0.9}Cl_{0.1}$, takes place during ball milling. A higher degree of dissolution of NaCl in $NaBH_4$ is obtained by annealing resulting in solid solutions containing up to 57 mol% NaCl, i.e. $Na(BH_4)_{0.43}Cl_{0.57}$. In addition, annealing results in dissolution of 10–20 mol% $NaBH_4$ into NaCl. The mechanism of the dissolution during annealing and the decomposition pathway of the solid solutions are studied by *in situ* SR-PXD. Furthermore, the stability upon hydrogen release and uptake were studied by Sieverts measurements.

1. Introduction

Developments of new environmentally friendly energy concepts are essential for the future of the modern industrialized society and hydrogen has been suggested as a future carrier of renewable energy. Unfortunately, storage of hydrogen remains an unsolved and extremely challenging task for a future hydrogen economy, especially for utilization of hydrogen in mobile applications. Solid state hydrogen storage as light element hydrides is a potential solution, which may provide sufficiently high energy density and efficiency [1,2]. Within this class of materials, the metal borohydrides have received increasing interest in the past decade due to their high gravimetric and volumetric hydrogen densities. Unfortunately, many of these materials are too stable, i.e. decompose at too high temperatures for practical applications [3–5]. Therefore, much research has focused on synthesis of novel materials and on altering the properties of known materials [6].

A wide range of novel metal borohydrides have been synthesized and characterized structurally, physically and chemically. An empirical correlation between the decomposition temperature or the enthalpy of formation and the Pauling electronegativity of the cation has been found [7]. The studies of the novel metal borohydrides suggest that the introduction of some degree of covalent character in the M–BH_4 interaction facilitates release of hydrogen at lower temperatures and also the formation of more open structures [5], e.g. $Mg(BH_4)_2$ [8], $Mn(BH_4)_2$ [9] and $Y(BH_4)_3$ [10–12]. This also holds for a range of new bimetal borohydrides, e.g. $MSc(BH_4)_4$ (M=Li, Na and K) [13–16], $NaZn(BH_4)_3$, $MZn_2(BH_4)_5$ (M=Li or Na) [17] as well as the first structurally ordered heteroleptic borohydride, $KZn(BH_4)Cl_2$ [18].

One approach to improve the properties of known borohydrides is by chemical reactions as realized for reactive hydride composites, for which the thermodynamic properties may be significantly improved as observed for the $2LiBH_4$–MgH_2 system [19–24]. Furthermore, the kinetic and possibly also thermodynamic properties of reactive hydride composites can be improved by nanoconfinement or using catalytically active additives [25–27].

A recently developed method suggested for altering the thermodynamic properties of borohydride materials is anion substitution, where a halide anion i.e. F^-, Cl^-, Br^- or I^- is substituted for either H^- or BH_4^- in the metal borohydride structure. Fast dissolution of lithium chloride in the hexagonal structure of lithium borohydride, h-$LiBH_4$ followed by slow segregation of lithium chloride from the solid solution $Li(BH_4)_{1-x}Cl_x$ was recently observed [28,29]. The heavier halides appear to stabilize lithium borohydride, however, theoretical studies suggest that the more electronegative fluoride ion may introduce destabilization [30]. Furthermore, three new solid solutions have been found in the $Ca(BH_4)_2$–CaI_2 system [31].

Dissolution of MCl into MBH_4, M=Li, Na or K, have also been observed in samples containing novel metal borohydrides synthesized by ball milling, where MCl or other chloride containing salts are formed as a byproduct, e.g. MCl is slowly dissolved in MBH_4 during the thermal decomposition of $MSc(BH_4)_4$, M=Na or K [15,16]. Therefore, anion substitution might also play an important role in the understanding of the thermal decomposition of the novel metal borohydrides in such samples.

* Corresponding author. Fax: +45 8619 6199.
E-mail address: trj@chem.au.dk (T.R. Jensen).

0022-4596/$ - see front matter © 2011 Elsevier Inc. All rights reserved.
doi:10.1016/j.jssc.2011.05.030

In this study we investigate the dissolution of NaCl in $NaBH_4$. We utilize two different dissolution methods: ball milling and annealing. The mechanism for the dissolution and the degree of anion substitution obtained by the different methods is studied by Rietveld refinement of synchrotron radiation powder X-ray diffraction (SR-PXD) data. Furthermore, the effect of the anion substitution on the thermal stability is studied by Sieverts measurements.

2. Experimental

2.1. Sample preparation

Samples of $NaBH_4$–NaCl in molar ratios of 0.5:0.5 and 0.75:0.25, denoted sample S1 and S2, respectively, and a sample containing only $NaBH_4$, denoted S3 were ball milled (BM) using the same conditions comprised of 60 times 2 min of milling each intervened by 2 min breaks to avoid heating of the samples. Ball milling was conducted under inert conditions (argon atmosphere) using a Fritsch Pulverisette P4 planetary mill using 80 mL tungsten carbide (WC) containers and a sample to balls mass ratio of approximately 1:35 (balls WC, o.d. 10 mm). After ball milling, approximately 0.5 g of each sample was transferred to a corundum (Al_2O_3) crucible, placed inside a sealed argon filled quartz capillary, and annealed in a furnace kept at a fixed temperature of 300 °C for 3 days. This is referred to as annealing (A). After annealing the samples are denoted S1A, S2A and S3A, respectively. Information about the sample composition and treatment is given in Table 1. The chemicals used were: $NaBH_4$ ($\geq$98.5%, Aldrich) and NaCl (>99.5%, Ferak). The preparation and manipulation of all samples were performed in an argon-filled glovebox with a circulation purifier.

2.2. In situ synchrotron radiation powder X-ray diffraction

In situ SR-PXD was collected at beamline I711 of the synchrotron MAX II, Lund, Sweden at the research laboratory MAX-Lab with a MAR165 CCD detector system and selected wavelengths of λ=0.945(2) or 1.072(2) Å [32]. The X-ray exposure time was 30 s. The sample cell was specially developed for studies of gas/solid reactions and allows elevated pressure and temperature to be applied. The powdered sample was mounted in a sapphire (Al_2O_3) single-crystal tube (o.d. 1.09 mm, i.d. 0.79 mm) in an argon-filled glovebox with a circulation purifier. The sample holder was sealed inside a glovebox. The temperature was controlled with a thermocouple placed in the sapphire tube 1 mm from the sample [33]. All obtained raw images were transformed to 2D-powder patterns using the FIT2D program [34], which was also used for calibration using measurements of the standard NIST LaB_6 sample and masking diffraction spots from the single-crystal sapphire sample holder. Uncertainties of the integrated intensities were calculated at each 2θ-point by applying Poisson statistics to the intensity data, considering the geometry of the detector [35].

For the study of the anion substitution mechanism, sample S1 was heated from *RT* to 300 °C, kept at this temperature for 30 min and cooled to 30 °C. Both heating and cooling were conducted with heating and cooling rates of 10 °C/min. This procedure was repeated three times in total in order to investigate the stability of the formed solid solutions. To study the effect of the anion substitution on the decomposition pathways samples S1A and S2A was heated from *RT* to 600 °C with a heating rate of 10 °C/min.

2.3. Laboratory powder X-ray diffraction (PXD)

In house PXD was measured for sample S1A 12 months after annealing. The sample had been stored in the glove box at room temperature (*RT*) during these 12 months. The PXD measurement was performed in Debye–Scherrer transmission geometry using a Stoe diffractometer equipped with a curved Ge(1 1 1) monochromator (Cu $K\alpha_1$ radiation) and curved position sensitive detector. Data were collected at *RT* between 4° and 127° 2θ with a counting time of ~960 s per step. The sample was mounted in a glovebox in a 0.5 mm glass capillaries sealed with glue.

2.4. Rietveld refinements

Rietveld refinements were performed using the Fullprof program [36]. The backgrounds were described by linear interpolation between selected points, while pseudo-Voigt profile functions were used to fit the diffraction peaks. In the refinements of single SR-PXD datasets at selected temperatures, unit cell parameters, zero shift, profile parameters and the overall temperature factors, B_{ov} were refined. The chloride substitution in sodium borohydride was modeled by introducing Cl on the position of B in $NaBH_4$ and the occupancies of Cl, B and H were refined. The overall occupancy of Cl and BH_4 was constrained to one. For the samples S1A and S2A the BH_4 substitution in NaCl was modeled in a similar way, introducing B on the position of Cl.

Table 1
Sample composition prior to treatment, utilized treatment to obtain anion substitution (BM: ball milling for 120 min, A: Annealed at 300 °C for 3 days), sample composition after treatment and unit cell parameter, *a* for the solid solutions, $NaBH_4$ and NaCl. Substitution degrees, mol%, wt% and unit cell parameter after treatments are determined by Rietveld refinement of SR-PXD data.

Sample	Before treatment			After treatment				
	Composition			Treatment	Composition			*a* (Å)
S1	$NaBH_4$	50 mol%	40 wt%	BM	$Na(BH_4)_{0.90}Cl_{0.10}$	50.3(5) mol%	40.9(5) wt%	6.1208(5)
	NaCl	50 mol%	60 wt%		NaCl	49.7(4) mol%	59.1(5) wt%	5.6421(3)
S1A	$NaBH_4$	50 mol%	40 wt%	BM+A	$Na(BH_4)_{0.43}Cl_{0.57}$	63.9(18) mol%	59.4(17) wt%	5.9579(2)
	NaCl	50 mol%	60 wt%		$Na(BH_4)_{0.10}Cl_{0.90}$	14.5(8) mol%	15.3(8) wt%	5.7800(11)
					NaCl	9.3(4) mol%	10.2(4) wt%	5.6876(7)
					$NaBO_2$	12.2(3) mol%,	15.1(4) wt%	–
S2A	$NaBH_4$	75 mol%	66 wt%	BM+A	$Na(BH_4)_{0.68}Cl_{0.32}$	80.0(12) mol%	74.6(11) wt%	6.03416(19)
	NaCl	25 mol%	34 wt%		$Na(BH_4)_{0.20}Cl_{0.80}$	8.9(4) mol%	10.1(5) wt%	5.6506(8)
					$NaBO_2$	11.1(4) mol%	15.3(6) wt%	–
S3	$NaBH_4$	100 mol%	100 wt%	BM	$NaBH_4$	100.0 mol%	100.0 wt%	6.15714(9)
S3A	$NaBH_4$	100 mol%	100 wt%	BM+A	$NaBH_4$	100.0 mol%	100.0 wt%	6.15928(11)

The hydrogen atoms were not included in the latter model, since they are very weak X-rays scatters and the orientation of BH_4 units i.e. the positions of the hydrogen might not be ordered.

For the *in situ* SR-PXD data measured for sample S1 a sequential refinement was carried out by splitting the data into two series of PXD no. 1 to 200 containing NaCl and $Na(BH_4)_{1-x}Cl_x$ and PXD no. 200 to 422 containing NaCl, $Na(BH_4)_{1-x}Cl_x$ and $NaBO_2$. Small amounts of $NaBO_2$ is observed before scan 200, however, the amounts are too small for reliable fits. The first pattern of each series was refined as described above, however, with all linearly interpolated background points varied and the preliminarily determined zero shifts fixed. For the sequential refinement all unit cell parameters, profile parameters, overall temperature factors, B_{ov} and occupancies of Cl, B and H in $Na(BH_4)_{1-x}Cl_x$ were refined.

The standard uncertainties of the occupancies given by the Rietveld refinements are unrealistically low, i.e. below 1% of the refined values. These are likely to be higher mainly due to the correlation between the occupancies and the atomic temperature factors not being taken into account. Therefore the standard uncertainties of the substitution degrees are not given. Furthermore, the sample compositions extracted by Rietveld refinement are only approximate, since these might be affected by presence of amorphous phases and/or micro-adsorption.

2.5. Sieverts measurements

Sieverts measurements (temperature programmed desorption, TPD) were recorded for samples S1A, S3 and sample S3A using a PCTpro 2000 instrument from Hy-Energy [37]. The samples were loaded in an autoclave and sealed in argon atmosphere. For the first TPD experiment for each sample, a multistep temperature program was used i.e. the sample was heated from *RT* to 450 °C with a heating rate of 0.5 °C/min followed by a dwell time of 10 h at 450 °C. Subsequently, the samples were heated to 500 °C with a heating rate of 200 °C/min followed by a dwell time of 25 h at 500 °C. At last, the samples were heated to 550 °C with a heating ramp of 200 °C/min and the measurement was continued at 550 °C until desorption was completed. The second and third TPD experiments were performed with a continuous temperature program from *RT* to 550 °C using a heating rate of 0.5 °C/min. For all desorption experiments a hydrogen back pressure of 1 bar was used to suppress the formation of diborane. Hydrogen absorptions were conducted at a fixed temperature of 450 °C for 40–94 h. A hydrogen pressure of ca. 90 bar was initially applied.

3. Results and discussion

3.1. Substitution methods

Anion substitution is obtained using two different methods: ball milling (sample S1) or ball milling and annealing, i.e. heating the samples at a fixed temperature of 300 °C for 3 days (samples S1A and S2A). The samples were examined by Rietveld refinement of SR-PXD data (Table 1).

The ball milled sample $NaBH_4$–NaCl (0.5:0.5, S1) reveals substitution of chloride into the structure of sodium borohydride, i.e. formation of a solid solution $Na(BH_4)_{1-x}Cl_x$ (Fig. 1a). The anion substitution causes a decrease in the unit cell parameter, due to the smaller ionic radii of Cl^- (1.81 Å) as compared to that of BH_4^- (2.05(19) Å) [38], i.e. the cell parameter for the $Na(BH_4)_{1-x}Cl_x$ is found to be $a=6.1208(5)$ Å. In comparison the unit cell parameter found in a sample of ball milled $NaBH_4$ (S3) is $a=6.15714(9)$ Å (Fig. 1d). Furthermore, significant changes in the relative peak intensities are observed in the PXD data and dissolution of 10 mol% NaCl in $NaBH_4$ is clearly observed, i.e. the composition of the solid solution formed by ball milling is $Na(BH_4)_{0.90}Cl_{0.10}$. This reflects that a reaction according to reaction scheme (1) takes place during ball milling.

$$(1-x)NaBH_4 + xNaCl \rightarrow Na(BH_4)_{1-x}Cl_x \quad (1)$$

Reflections from NaCl exhibit similar 2θ position and intensity as compared to the sample prior to ball milling, which suggests that no or very limited amounts of $NaBH_4$ is dissolved in NaCl during ball milling.

Rietveld refinement of SR-PXD data measured for sample S1 using a model without chloride substitution was also conducted but resulted in a poorer fit giving agreement factors of $R_p=8.43$ and $R_{wp}=10.3$ as compared to those for the model implementing chloride substitution of $R_p=4.55$ and $R_{wp}=5.73$ (corrected for background). Furthermore, a Rietveld model implementing BH_4 substitution in NaCl was also tried for sample S1, however, the occupancy of Cl refined to close to zero, i.e. no measurable substitution of $NaBH_4$ in NaCl was observed due to ball milling.

The SR-PXD data and Rietveld refinement of the annealed $NaBH_4$–NaCl (0.5:0.5, S1A) sample (S1A) is shown in Fig. 1b. Visual inspection of the SR-PXD data, Fig. 1a and b, suggests significant differences between the two samples S1 and S1A, prepared by ball milling and annealing, respectively. The chloride substituted sodium borohydride is found to have a unit cell parameter of $a=5.9579(2)$ Å and the composition $Na(BH_4)_{0.43}Cl_{0.57}$, i.e. more than half the anions in this solid solution are Cl^-. This suggests that the formation of the solid solution by reaction scheme (1) is more efficiently induced by heating (annealing) than by pressure (ball milling).

In addition, a substitution of BH_4^- into NaCl is also found to have occurred in sample S1A according to reaction scheme (2).

$$yNaCl + (1-y)NaBH_4 \rightarrow Na(BH_4)_{1-y}Cl_y \quad (2)$$

This results in a solid solution of composition $Na(BH_4)_{0.10}Cl_{0.90}$. The unit cell parameter of $a=5.886(3)$ Å is significantly larger than that found for the unsubstituted NaCl of $a=5.6421(3)$ Å (refined value using SR-PXD data for sample S1 at *RT*). The Bragg peaks originating from $Na(BH_4)_{0.10}Cl_{0.90}$ are relatively broad, indicating that the degree of substitution is distributed with an average composition $y=0.90$.

The fact that BH_4^- substitution in NaCl is not observed in the ball milled samples prior to annealing suggests that this process is less favorable compared to Cl^- substitution into $NaBH_4$, which is more favorable and hence occurs during ball milling. This might be due to the larger radii of BH_4^- compared to Cl^- i.e. the compound with the smaller anion, NaCl is more easily dissolved in the compound with the larger anion, $NaBH_4$. This causes contraction of the unit cell and increased lattice energy.

Only 9.3 mol% unsubstituted NaCl is present in sample S1A, i.e. the annealing causes the substitution reactions (reaction schemes (1) and (2)) to take place to a high extent. Furthermore, sodium borate, $NaBO_2$ is observed to form (12.1 mol%) during annealing. This may be due to water and/or oxygen contamination of the sample. This may possibly be avoided by thoroughly drying the starting materials prior to sample preparation to avoid presence of hydrous compounds such as $NaBH_4 \cdot 2H_2O$ [39].

In order to investigate possible full substitution (100%), i.e. formation of a single homogeneous solid solution, a sample containing 25 mol% NaCl (see Table 1) was ball milled and annealed (sample S2A) in a similar fashion as sample S1A. The Rietveld refinement of the SR-PXD data shown in Fig. 1c reveal formation of two solid solutions of composition $Na(BH_4)_{0.68}Cl_{0.32}$ (80 mol%) and $Na(BH_4)_{0.20}Cl_{0.80}$ (8 mol%) with unit cell parameters of $a=6.03416(19)$ and 5.6505(5) Å, respectively. Again, $NaBO_2$ have formed (12 mol%). It is interesting that BH_4^- substitution into NaCl is observed even though only 32 mol% Cl^- is substituted into $NaBH_4$, which is far less than the 57 mol%

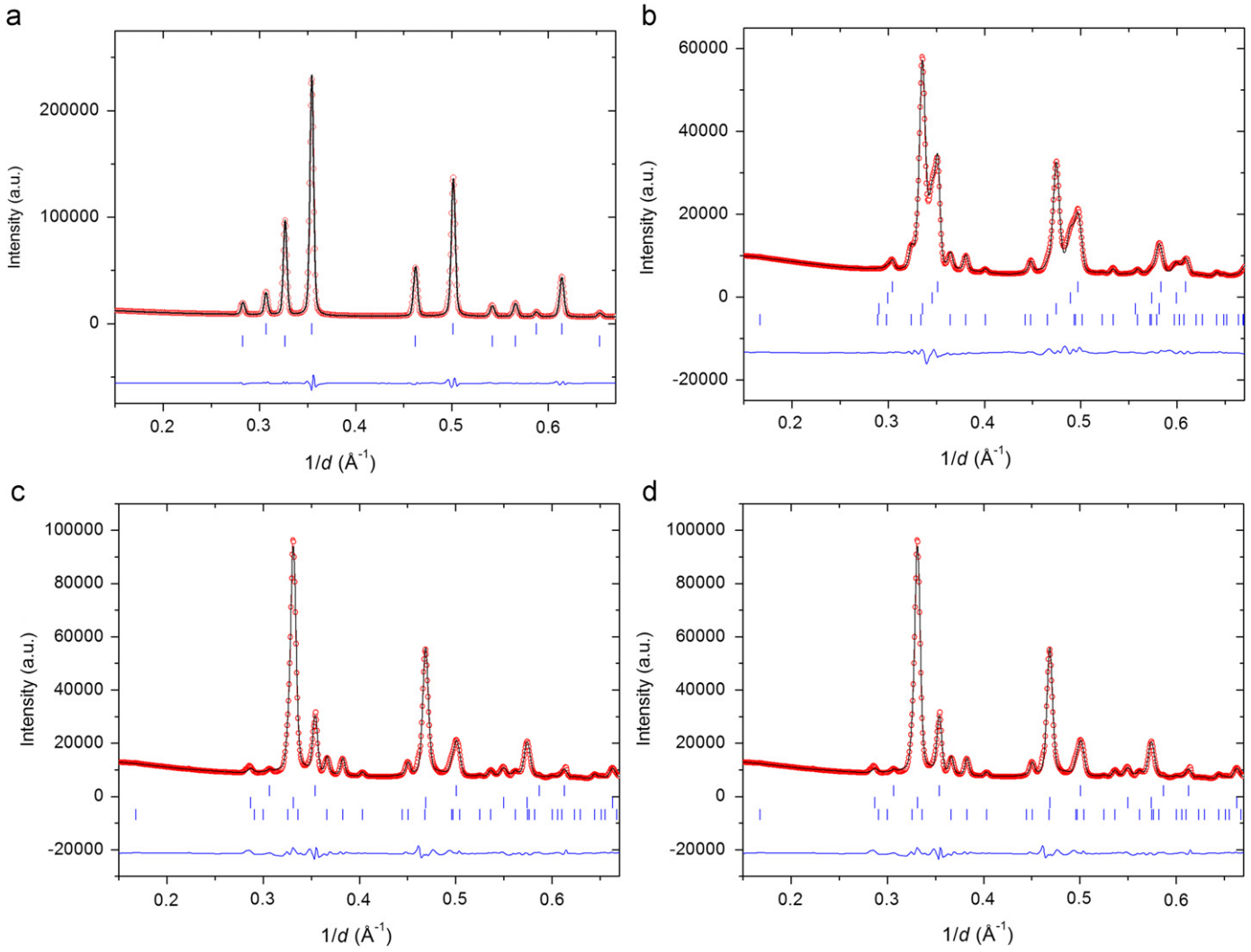

Fig. 1. SR-PXD data measured at *RT* and Rietveld refinement profiles plotted as a function of 1/*d* for (a) $NaBH_4$–NaCl (0.5:0.5, S1, λ=1.072(2) Å), (b) $NaBH_4$–NaCl (0.5:0.5, S1A, λ=0.945(2) Å), (c) $NaBH_4$–NaCl (0.75:0.25, S2A, λ=0.945(2) Å) and (d) $NaBH_4$ (S3, λ=0.945(2) Å). Circles: SR-PXD data (Y_{obs}); Upper curves: Rietveld refinement profiles (Y_{calc}); Lower curves: Residual (Y_{obs}–Y_{calc}); Marks: (from top) in (a): NaCl and $Na(BH_4)_{0.90}Cl_{0.10}$, (b): NaCl, $Na(BH_4)_{0.10}Cl_{0.90}$, $Na(BH_4)_{0.43}Cl_{0.57}$ and $NaBO_2$, (c): $Na(BH_4)_{0.20}Cl_{0.80}$, $Na(BH_4)_{0.68}Cl_{0.32}$ and $NaBO_2$ and (d): $NaBH_4$.

observed for sample S1A. This suggests, that substitution of Cl^- for BH_4^- in $NaBH_4$ is a fast process as compared to BH_4^- substitution in NaCl and that both reactions are diffusion limited. This likely means, that the smaller amount of NaCl in the sample, the smaller amount of Cl^- substitution into $NaBH_4$, before BH_4^- substitution into NaCl is initiated. This suggests that prolonged annealing may produce a single homogeneous solid solution $Na(BH_4)_{1-x}Cl_x$. However, the fact that this is not obtained by annealing at 300 °C for 3 days suggests that the diffusion of the anions is relatively slow.

Fig. 2 shows a plot of the observed unit cell parameters of $Na(BH_4)_{1-x}Cl_x$ solid solutions at *RT* as a function of substitution degree, *x*. The plot shows an approximate linear relationship according to Vegard's law. It should be noted that this relationship is only approximate due to the difficulty of determining the exact composition of the solid solutions due to correlation between the occupancies and the atomic temperature factors. In contrast, the unit cell parameters are very reliable experimental observations. However, unit cell parameters of the solid solutions formed from dissolution of $NaBH_4$ into NaCl is not included, since

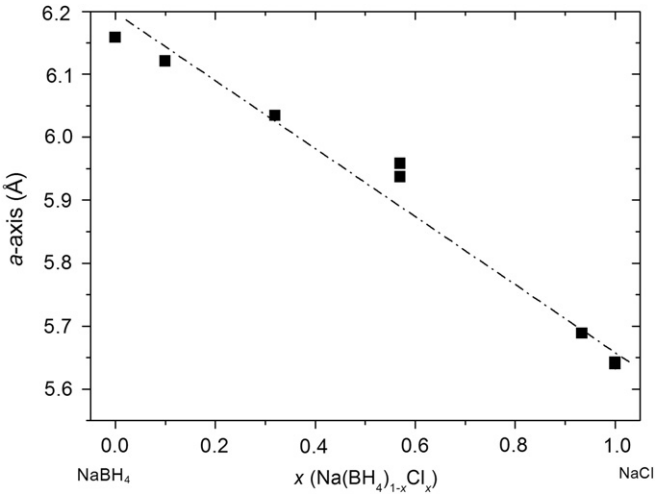

Fig. 2. Observed unit cell parameters of $Na(BH_4)_{1-x}Cl_x$ solid solutions at *RT* as a function of substitution degree, *x*.

they exhibit broad Bragg reflections lying close to those of NaCl, i.e. the cell parameters are likely to be less accurate.

For the annealed sample $NaBH_4$–NaCl (0.5:0.5, S1A) in house PXD data was measured 12 month after annealing in order to investigate possible solid state phase segregation. The sample still contains NaCl and two solid solutions: $Na(BH_4)_{1-x}Cl_x$ and $Na(BH_4)_{1-y}Cl_y$ with $y > x$. The relative small amount of $NaBO_2$ observed in the SR-PXD data is not observed in the in house PXD data. The quality of the data is not sufficient to determine the degree of substitutions, x and y however, the cell parameters, determined by Rietveld refinement, are found to be similar to those observed directly after annealing. This suggests that no significant phase segregation is taking place, which is in contrast to the significant phase segregation observed for solid solutions $Li(BH_4)_{1-x}Cl_x$, for which x decreases from 0.42 to 0.09 during 13 month at *RT* [29].

3.2. Mechanism for anion substitution

In order to investigate the mechanism of the substitution process during annealing, the ball milled sample $NaBH_4$–NaCl (0.5:0.5, S1) was investigated by *in situ* SR-PXD during three consecutive cycles of heating to 300 °C, annealing for 30 min and cooling to *RT*. The obtained data are shown in Fig. 3. The unit cell volumes of NaCl and the solid solution $Na(BH_4)_{1-x}Cl_x$, obtained by Rietveld refinement of 422 PXDs, are shown as a function of time together with the temperature profile for the experiment in Fig. 4.

As the temperature of the sample is changed, the unit cell volume of NaCl increases and decreases linearly due to thermal expansion and contraction, respectively. The linear thermal expansion coefficients, α for NaCl during the first heating ramp is $2.562(6)\times10^{-4}\,K^{-1}$ (T=32–300 °C). The reported α for the same temperature range is $2.515(4)\times10^{-4}\,K^{-1}$ (calculated from the equation for cell parameter, a for NaCl as a function of T reported by Pathak and Vasavada [40]). No changes are observed in the unit cell volume of NaCl during the three annealing, i.e. the unit cell volumes at T=32 °C at the start and end of the experiment are identical (179.606(4) and 179.599(13) Å^3, respectively). This suggests that no dissolution of $NaBH_4$ into NaCl takes place during the short time of the experiment (only 90 min at 300 °C).

An initial expansion of the unit cell volume is also observed for $Na(BH_4)_{1-x}Cl_x$ during the first heating ramp from 32 to ~240 °C. As the temperature reaches 240 °C during the first heating ramp, the unit cell volume of $Na(BH_4)_{1-x}Cl_x$ decreases rapidly and continues to do so for approximately 20 min. In this time range the unit cell parameter is found to decrease from 6.2099(3) to 6.1295(7) Å, while the degree of substitution, x changes from approximately 0.15 to 0.50. However, it should be noted that the substitution degrees at elevated temperatures obtained from Rietveld refinement are only approximate due to the correlation between the occupancies and the atomic temperature factors.

During the last 10 min of the first annealing period at 300 °C the substitution rate decreases significantly and reaches a plateau value, i.e. the decrease in unit cell volume of $Na(BH_4)_{1-x}Cl_x$ becomes linear. During the second and third annealing periods at 300 °C the unit cell volume of $Na(BH_4)_{1-x}Cl_x$ decreases linearly with similar rates. By fitting linear equations to the change in unit cell parameter during these annealing periods (PXD no. 58–85, 165–208 and 289–332 corresponding to t=46–57, 112–142 and 197–226 min, respectively), the unit cell parameter change is found to be $-5.53(8)\times10^{-4}$ Å/min. By relating this to the unit cell volume change as a function of substitution degree (from Fig. 2) the rate of NaCl substitution into $NaBH_4$ at 300 °C is found to be 0.105(3) mol% Cl/min. By similar calculations for the fast substitution during the first 20 min of the first annealing period (PXD no. 36–47 corresponding to t=24–32 min), the initial substitution rate is found to be 1.48(8) mol% Cl/min.

During the temperature ramps expansion and contraction of the solid solution $Na(BH_4)_{1-x}Cl_x$ is observed. The linear thermal expansion coefficient, α (T=32–200 °C) is found to decrease with the increasing degree of substitution, x, i.e. $\alpha=5.07(2)\times10^{-4}$, $4.828(18)\times10^{-4}$, $4.70(3)\times10^{-4}$ and $4.55\times10^{-4}\,K^{-1}$ for the four ramping periods (t=0–17, 68–102, 152–186 and 236–253 min, respectively). For comparison, the linear thermal expansion coefficient for $NaBH_4$ (extracted by Rietveld refinement of the *in situ*

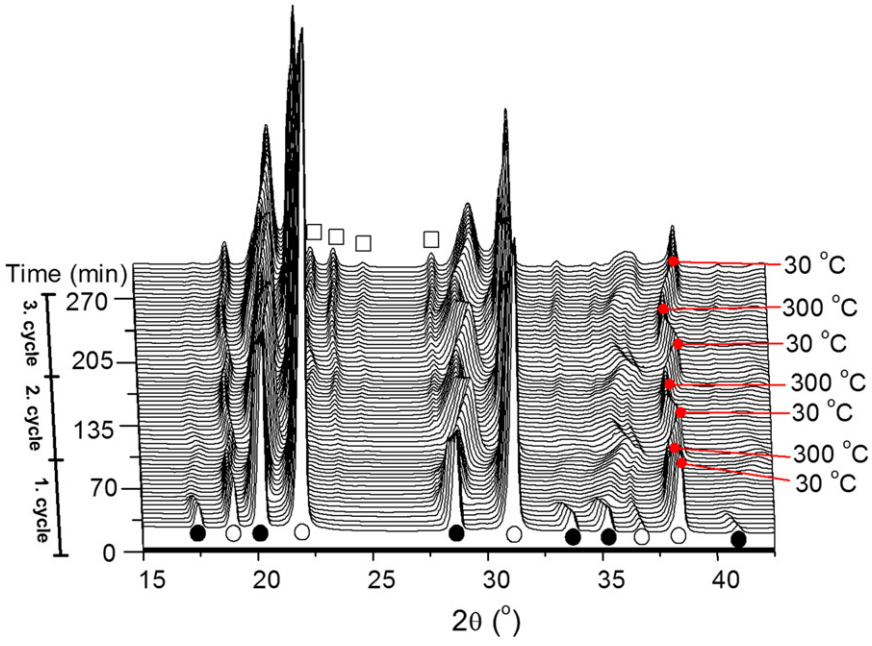

Fig. 3. *In situ* SR-PXD data for BM $NaBH_4$–NaCl (S1, 0.5:0.5) heated from *RT* to 300 °C, kept at 300 °C for 30 min, cooled from 300 to 30 °C ($\Delta T/\Delta t$=10 °C/min). This is repeated by three cycles. Symbols: ○ NaCl, ● $NaBH_4$ and □ $NaBO_2$ (λ=1.072(2) Å).

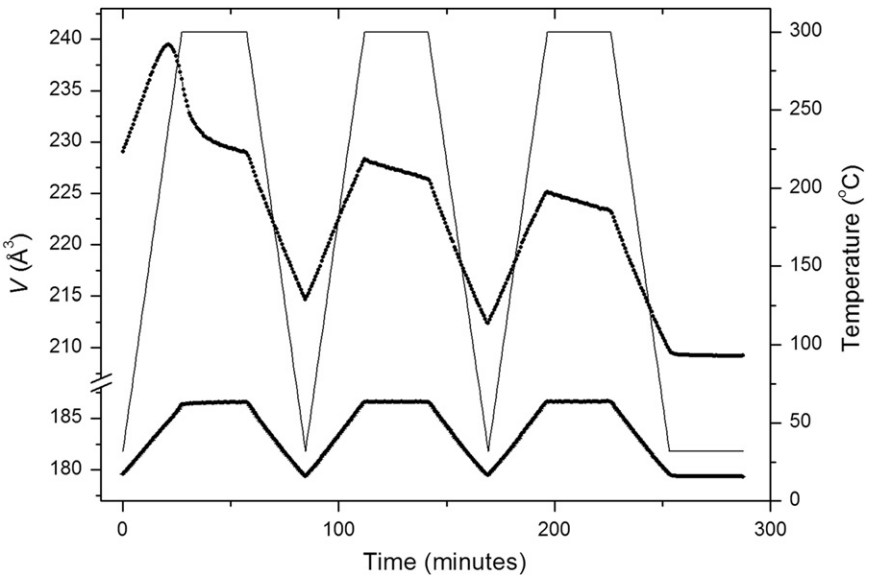

Fig. 4. Unit cell volumes for NaCl (lower curve) and the solid solution $Na(BH_4)_{1-x}Cl_x$ (upper curve) shown as function of time. The data are extracted from the *in situ* SR-PXD data shown in Fig. 3 by Rietveld refinement. The temperature profile for the experiment is shown as the thin curve.

SR-PXD measured on sample S3, see Fig. 5b) is found to be $5.36(6)\times10^{-4}\,K^{-1}$ (T=46–200 °C). Furthermore, the fact that the decrease in unit cell volume of $Na(BH_4)_{1-x}Cl_x$ is linear upon cooling suggests that NaCl do not segregate from $NaBH_4$ on the time scale of the experiment.

At *RT* after the third annealing period the unit cell parameter of the solid solution has decreased to 5.9368(8) Å and the final composition is found to be $Na(BH_4)_{0.43}Cl_{0.57}$. Interestingly, the final composition of the solid solution, $Na(BH_4)_{0.43}Cl_{0.57}$ is the same as in the annealed sample, S1A. However, in the latter sample substitution of BH_4 into NaCl was also observed. This suggests that substitution of BH_4^- into NaCl is slower than substitution of Cl^- into $NaBH_4$. This is likely due to limited solid state diffusion of the bigger anion, BH_4^- compared to that of Cl^-. However, different nucleation and growth rates of the two solid solutions might also hamper the substitution of BH_4^- into NaCl.

3.3. Effect of substitution on thermal decomposition

The decomposition pathway for the solid solution $Na(BH_4)_{1-x}Cl_x$ was investigated using *in situ* SR-PXD measurements conducted on the annealed $NaBH_4$–NaCl samples (S1A and S2A) and on the ball milled $NaBH_4$ (S3) for comparison. Fig. 5a and b shows the *in situ* SR-PXD for sample S1A and S3, respectively. The *in situ* SR-PXD data for the thermal decomposition of sample S2A is similar to that of sample S1A and is not included.

In situ SR-PXD data (Fig. 5b) for the ball milled $NaBH_4$ (S3) reveal formation of $NaBO_2$ at ~300 °C. At ~495 °C the diffraction from $NaBH_4$ decreases rapidly and vanishes due to melting and thermal decomposition. At this temperature the diffraction from $NaBO_2$ also vanishes, possibly due to dissolution in the $NaBH_4$ melt. No diffraction is observed from decompositions products. However, metallic Na might have formed as a dehydrogenation product from $NaBH_4$ due to the lack of a hydrogen back-pressure during the dehydrogenation (NaH is reported to decompose at ~425 °C [3]). Sodium (T_m=98 °C, T_b=883 °C) might evaporate at the relative high temperatures. The decomposition facilitates a significant decrease in the background intensity, which indicates that less material is exposed to the X-ray beam.

The sample of $NaBH_4$–NaCl (0.5:0.5, S1A) after ball milling and annealing contains as mentioned two solid solutions: $Na(BH_4)_{0.43}Cl_{0.57}$ and $Na(BH_4)_{0.1}Cl_{0.9}$, besides NaCl and $NaBO_2$. The

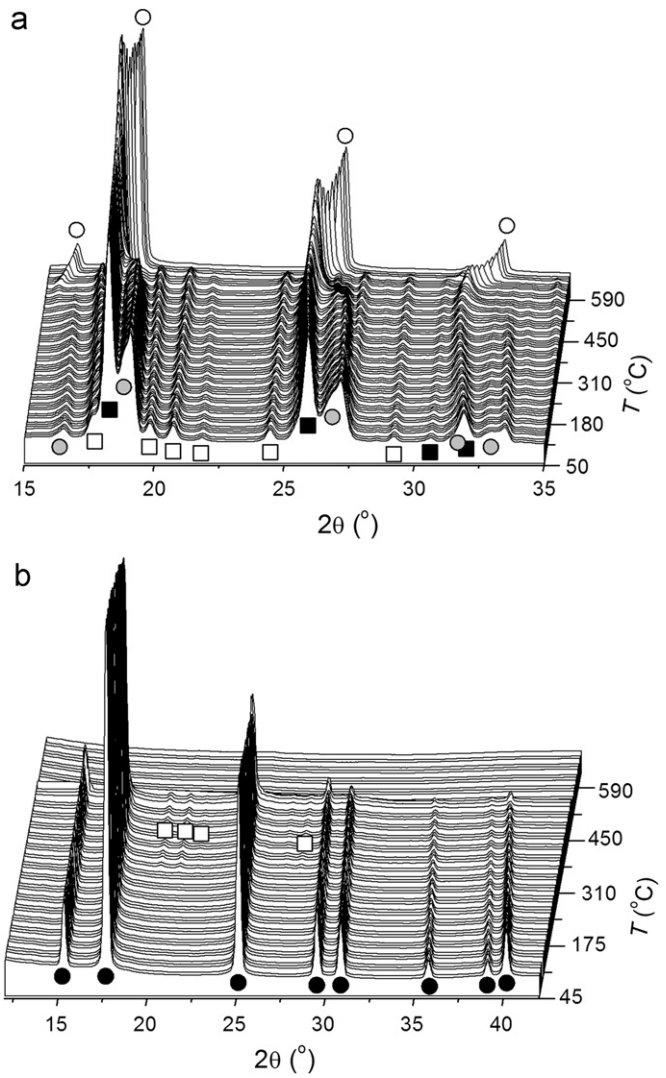

Fig. 5. *In situ* SR-PXD data for (a) $NaBH_4$-NaCl (0.5:0.5, S1A) and (b) $NaBH_4$ (S3) measured from *RT* to 600 °C ($\Delta T/\Delta t$=10 °C/min). Symbols: ◯ $Na(BH_4)_{1-x}Cl_x$, ■ $Na(BH_4)_{1-y}Cl_y$, ○ NaCl, ● $NaBH_4$ and □ $NaBO_2$ (λ=0.945(2) Å).

diffracted intensity from NaCl shows a slow increase starting at ~380 °C, simultaneously with broadening and small changes in the 2θ positions of the Bragg peaks from the two solid solutions. In fact, the Bragg peaks from the two solid solutions move towards each other and tend to merge at temperatures $T > 350$ °C. This indicates that a relatively fast solid state diffusion takes place and that prolonged annealing at this temperature might result in formation of a single homogeneous solid solution. As the temperature reaches ~380 °C the diffracted intensity from NaCl decrease, i.e. is consumed by dissolution into the solid solutions and the diffracted intensity from both $Na(BH_4)_{1-x}Cl_x$ and $Na(BH_4)_{1-y}Cl_y$ increase rapidly. Upon further heating ($T > 415$ °C) the compositions of the two cubic solid solutions changes fast, i.e. the unit cell parameter, a for $Na(BH_4)_{1-x}Cl_x$ decreases due to increasing Cl^- content, while a for $Na(BH_4)_{1-y}Cl_y$ increases due to increasing BH_4^- content. At ~500 °C only one $Na(BH_4)_{1-x}Cl_x$ solid solution is present with relatively narrow Bragg peaks, indicating that the solid solution is relatively homogeneous. At ~530 °C $Na(BH_4)_{1-x}Cl_x$ begins to decompose simultaneously with disappearing of the $NaBO_2$ peaks. The decomposition results in changes of the 2θ peak positions towards those for NaCl, which is due to extraction of $NaBH_4$ from the solid solution. Sodium borohydride likely melts, dissolve $NaBO_2$ and decompose to amorphous boron and molten sodium, which may partly evaporate. After the temperature reached 600 °C, the sample was cooled to *RT* and the remaining solid solution was found to consists of 6.7 mol% BH_4^-, i.e. the composition is $Na(BH_4)_{6.7}Cl_{93.4}$.

3.4. Hydrogen release and uptake in the solid solution

Sieverts measurements were used to investigate the hydrogen release and uptake for the annealed $NaBH_4$–NaCl (0.5:0.5, S1A) and for comparison; ball milled $NaBH_4$ (S3) and annealed $NaBH_4$ (S3A). The results are summarized in Table 2.

The first desorption measurement (TPD) is shown in Fig. 6. For the annealed $NaBH_4$ (S3A) a total hydrogen release of 2.6 wt% is observed. This corresponds to 32% of the calculated capacity, $\rho_m(H_2) = 7.992$ wt%. The majority of the gas-release is observed in the temperature range from 500 to 550 °C, however, a small amount of gas is released in the temperature range from *RT* to 300 °C. A sample of ball milled $NaBH_4$ (S3) was measured for comparison. A release of 3.6 wt% (45% of the calculated capacity) is observed for the same period of time (60 h). After 108 h a total of 6.6 wt% is released from the ball milled $NaBH_4$ (S3).

The sample of annealed $NaBH_4$–NaCl (0.5:0.5, S1A) shows a first desorption of 1.92 wt% hydrogen release after 60 h of measurement ($T \leq 550$ °C). This corresponds to 61% of the calculated capacity, $\rho_m(H_2) = 3.14$ wt%. It should be noted that the SR-PXD measurements as mentioned show that a small amount of $NaBO_2$ forms during annealing. Hence release of the full calculated hydrogen capacity for this sample cannot be expected.

The properties for the cycling of hydrogen release and uptake were investigated by rehydrogenation of the annealed $NaBH_4$ (S3A) and the sample of annealed $NaBH_4$–NaCl (0.5:0.5, S1A) and subsequently measuring the temperature desorption profiles. Two such cycles were performed for each sample, i.e. the second and third desorptions were measured (see Fig. 7). The annealed $NaBH_4$ (S3A) shows gas release of 1.2 and 1.0 wt% (15% and 13% of the calculated capacity) for the second and third desorptions, respectively. The second hydrogen desorption measurement performed for the annealed $NaBH_4$–NaCl (0.5:0.5, S1A) shows a

Table 2
Calculated hydrogen content, $\rho_m(H_2)$ and observed hydrogen release measured by the Sieverts method for annealed $NaBH_4$ (S3A), ball milled $NaBH_4$ (S3) and annealed $NaBH_4$-NaCl (0.5:0.5, S1A). The observed hydrogen release is shown for three consecutive TPD measurements. The percentage of the full capacity and the absorption time is written in the brackets. Experiments with a complete desorption is denoted END.

Sample	$\rho_m(H_2)$ (wt%)[a]	Cycle 1 obs. mass loss (wt%)		Cycle 2 obs. mass loss (wt%)	Cycle 3 obs. mass loss (wt%)
		60 h	END	END	END
$NaBH_4$ (S3A)	7.99	2.6 (32%)	–	1.2 (15%, Abs 47 h)	1.0 (13%, Abs 74 h)
$NaBH_4$ (S3)	7.99	3.6 (45%)	6.6 (82%)	1.2 (15%, Abs 60 h)	1.4 (18%, Abs 56 h)
$NaBH_4$–NaCl (S1A)	3.14	1.9 (61%)	1.9 (61%)	2.8 (90%, Abs 94 h)	2.3 (74%, Abs 45 h)

[a] Assuming the decomposition reaction: $NaBH_4 \rightarrow NaH + B + 3/2H_2$.

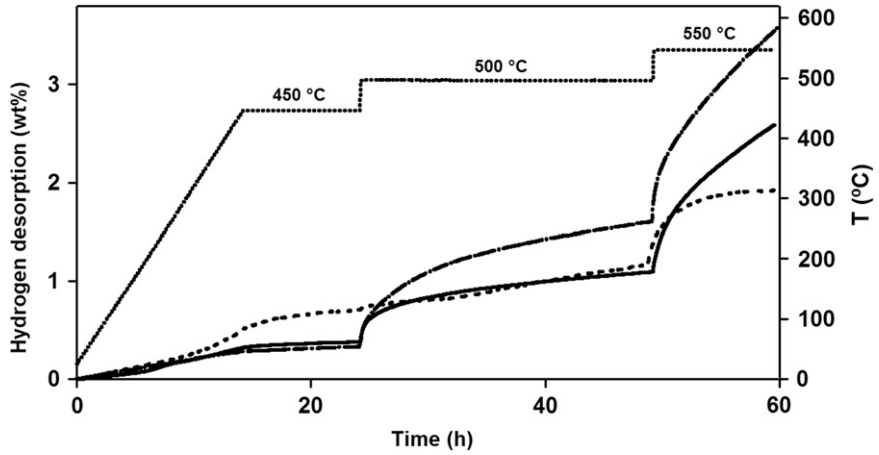

Fig. 6. Temperature pressure desorption measurement of the 1. desorption cycle, conducted from *RT* to 450 °C ($\Delta T/\Delta t = 0.5$ °C/min) for annealed $NaBH_4$ (S3A, solid line), ball milled $NaBH_4$ (S3, dot-dash) and $NaBH_4$-NaCl (0.5:0.5) (S1A, dashed line). The temperature profile is shown as dots. The hydrogen release (wt%) is shown on the left axis and the temperature scale on the right.

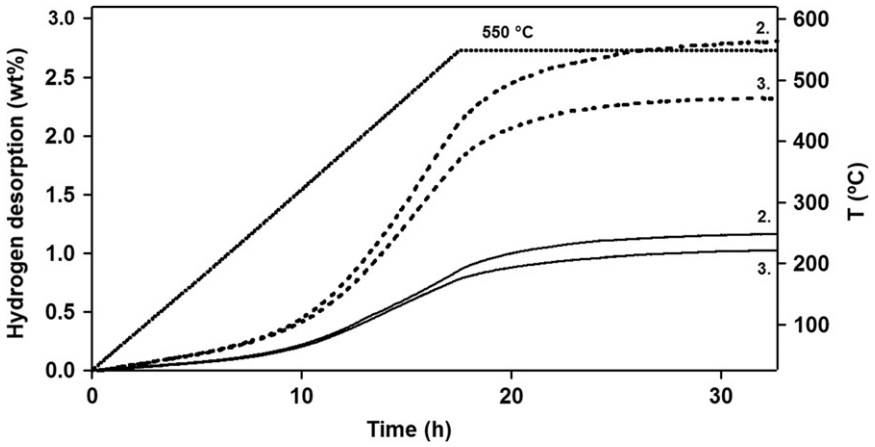

Fig. 7. Temperature pressure desorption measurement of the 2 and 3 desorption cycles, conducted from *RT* to 450 °C ($\Delta T/\Delta t = 0.5$ °C/min) for annealed $NaBH_4$ (S3A, solid line) and $NaBH_4$–NaCl (0.5:0.5) (S1A, dashed line). The temperature profile is shown as dots. The hydrogen release (wt%) is shown on the left axis and the temperature scale on the right.

total hydrogen release of 2.8 wt% (90% of the calculated capacity). Thus the hydrogen release is greater in the second cycle compared to the first, indicating that some hydrogen was released during the annealing at 300 °C performed prior to the Sieverts measurements. The third desorption shows a release of 2.3 wt% H_2 (74% of the calculated capacity), which is a decrease compared to the second cycle. This indicates that either the sample was not fully loaded with hydrogen during the 45 h of absorption or that the reversibility is reduced with the number of hydrogen release/uptake cycles performed.

4. Conclusion

Chloride substitution in sodium borohydride is investigated in samples of $NaBH_4$–NaCl. The substitution has been obtained by mechanical (ball milling) and thermal (annealing) treatment and the resulting solid solutions, $Na(BH_4)_{1-x}Cl_x$ have been studied by SR-PXD. Ball milling causes formation of $Na(BH_4)_{0.90}Cl_{0.10}$, while prolonged annealing results in solid solutions of higher Cl^- contents, e.g. $Na(BH_4)_{0.43}Cl_{0.57}$. This suggests that the formation of the solid solution is more efficiently induced by heating (annealing) than by mechanical treatment (pressure). Furthermore, prolonged annealing results in dissolution of $NaBH_4$ into NaCl. The *in situ* SR-PXD study of the substitution mechanism shows that fast dissolution of NaCl into $NaBH_4$ is initiated at ~240 °C and that the substitution rate decreases after 20 min of annealing at 300 °C, after which substitution proceeds at a constant rate. These studies also indicate that the substitution of BH_4^- into NaCl is taking place at a much lower rate. Investigation of the decomposition pathway of the $Na(BH_4)_{1-x}Cl_x$ solid solutions shows that at higher temperature, i.e. ~415 °C the rate of solid state diffusion is significantly increased such that a single and homogeneous solid solution is formed before slow decomposition of the $NaBH_4$–part of the solid solution at ~530 °C.

Acknowledgment

The authors are grateful to the Danish National Research Foundation (Centre for Materials Crystallography), the Danish Strategic Research Council (Centre for Energy Materials), The European Commission (contract NMP-2008-261/FLYHY), the Danish Research Council for Nature and Universe (Danscatt) and the Carlsberg Foundation for funding. We thank the staff of beamline I711, MAX-Lab for experimental support and for providing the beam time.

References

[1] L. Schlapbach, Nature 460 (2009) 809.
[2] S.-I. Orimo, Y. Nakamori, J.R. Eliseo, A. Züttel, C.M. Jensen, Chem. Rev. 107 (2007) 4111.
[3] W. Grochala, P.P. Edwards, Chem. Rev. 104 (2004) 1283.
[4] A. Züttel, S. Rentsch, P. Fischer, P. Wenger, P. Sudan, Ph. Mauron, Ch. Emmenegger, J. Alloys Compd. 356–357 (2003) 515.
[5] D.B. Ravnsbæk, Y. Filinchuk, R. Černý, T.R. Jensen, Z. Kristallogr. 225 (2010) 557.
[6] L.H. Rude, T.K. Nielsen, D.B. Ravnsbæk, U. Bösenberg, M.B. Ley, B. Richter, L.M. Arnbjerg, M. Dornheim, Y. Filinchuk, F. Besenbacher and T.R. Jensen, Phys. Status Solidi, in press, doi:pssc.201001214.R1.
[7] Y. Nakamori, K. Miwa, A. Ninomiya, H.-W. Li, N. Ohba, S. Towata, A. Züttel, S. Orimo, Phys. Rev. B 74 (2006) 045126.
[8] Y. Filinchuk, R. Černý, H. Hagemann, Chem. Mater. 21 (2009) 925.
[9] R. Černý, N. Penin, H. Hagemann, Y. Filinchuk, J. Phys. Chem. C 113 (2009) 9003.
[10] D.B. Ravnsbæk, Y. Filinchuk, R. Černý, M.B. Ley, D. Haase, H.J. Jakobsen, J. Skibsted, T.R. Jensen, Inorg. Chem. 49 (2010) 3801.
[11] C. Frommen, N. Aliouane, S. Deledda, J.E. Fonneløp, H. Grove, K. Lieutenant, I. Llamas-Jansa, S. Sartori, M.H. Sørby, B.C. Hauback, J. Alloys Compd. 496 (2010) 710.
[12] T. Jaron, W. Grochala, Dalton Trans. 39 (2010) 160.
[13] H. Hagemann, M. Longhini, J.W. Kaminski, T.A. Wesolowski, R. Černý, N. Penin, M.H. Sørby, B.C. Hauback, G. Severa, C.M. Jensen, J. Phys. Chem. A 112 (2008) 7551.
[14] S.-J. Hwang, R.C. Bowman, J.W. Reiter, J. Rijssenbeek, G.L. Soloveichik, J.-C. Zhao, H. Kabbour, C.C. Ahn, J. Phys. Chem. A 112 (2008) 3164.
[15] R. Černý, G. Severa, D.B. Ravnsbæk, Y. Filinchuk, V. d'Anna, H. Hagemann, D. Haase, C.M. Jensen, T.R. Jensen, J. Phys. Chem. C 114 (2010) 1357.
[16] R. Černý, D.B. Ravnsbæk, G. Severa, Y. Filinchuk, V. d'Anna, H. Hagemann, D. Haase, J. Skibsted, C.M. Jensen, T.R. Jensen, J. Phys. Chem. C 114 (2010) 19540.
[17] D. Ravnsbæk, Y. Filinchuk, Y. Cerenius, H.J. Jakobsen, F. Besenbacher, J. Skibsted, T.R. Jensen, Angew. Chem. Int. Ed. 48 (2009) 6659.
[18] D.B. Ravnsbæk, L.H. Sørensen, Y. Filinchuk, D. Reed, D. Book, H.J. Jakobsen, F. Besenbacher, J. Skibsted, T.R. Jensen, J. Eur. Inorg. Chem. 2010 (1608).
[19] J.J. Vajo, S.L. Skeith, F. Mertens, J. Phys. Chem. B 109 (2005) 3719.
[20] U. Bösenberg, S. Doppiu, L. Mosegaard, G. Barkhordarian, N. Eigen, A. Borgschulte, T.R. Jensen, Y. Cerenius, O. Gutfleisch, T. Klassen, M. Dornheim, R. Bormann, Acta Mater. 55 (2007) 3951.
[21] Y.W. Cho, J. Shim, B. Lee, CALPHAD 30 (2006) 65.
[22] U. Bösenberg, D.B. Ravnsbæk, H. Hagemann, V. D'Anna, C.B. Minella, C. Pistidda, W. van Beek, T.R. Jensen, R. Bormann, M. Dornheim, J. Phys. Chem. C 114 (2010) 15212.
[23] T.E.C. Price, D.M. Grant, V. Legrand, G.S. Walker, J. Int., Hydrogen Energy 35 (2010) 4154.
[24] T.E.C. Pricea, D.M. Granta, I. Telepenia, X.B. Yub, G.S. Walker, J. Alloys Compd. 472 (2009) 559.
[25] T.K. Nielsen, U. Bösenberg, R. Gosalawit, M. Dornheim, Y. Cerenius, F. Besenbacher, T.R. Jensen, ACS Nano, in press, doi:10.1021/nn1006946.
[26] U. Bösenberg, J.W. Kim, D. Gosslar, N. Eigen, T.R. Jensen, J.M. von Colbe, Y. Zhou, M. Dahms, D.H. Kim, R. Günther, Y.W. Cho, K.H. Oh, T. Klassen, R. Bormann, M. Dornheim, Acta Mater. 58 (2010) 3381.
[27] T.K. Nielsen, F. Besenbacher, and T.R. Jensen, Nanoscale (2011) 10.1039/C0NR00725K.
[28] L. Mosegaard, B. Møller, J.E. Jørgensen, Y. Filinchuk, Y. Cerenius, J.C. Hanson, E. Dimasi, F. Besenbacher, T.R. Jensen, J. Phys. Chem. C 112 (2008) 1299.
[29] L.M. Arnbjerg, D.B. Ravnsbæk, Y. Filinchuk, R.T. Vang, Y. Cerenius, F. Besenbacher, J.E. Jørgensen, H.J. Jakobsen, T.R. Jensen, Chem. Mater. 21 (2009) 5772.
[30] L. Yin, P. Wang, Z. Fang, H.M. Cheng, Chem. Phys. Lett. 450 (2008) 318.

[31] L.H. Rude, Y. Filinchuk, M.H. Sørby, B.C. Hauback, F. Besenbacher, T.R. Jensen, J. Phys. Chem. C (2011) 10.1021/jp111473d.
[32] Y. Cerenius, K. Ståhl, L.A. Svensson, T. Ursby, Å. Oskarsson, J. Albertsson, A. Liljas, J. Synch. Rad. 7 (2000) 203.
[33] T.R. Jensen, T.K. Nielsen, Y. Filinchuk, J.-E. Jørgensen, Y. Cerenius, E. Mac, A. Gray, C.J. Webb, J. Appl. Cryst. (2010) 43.
[34] A.P. Hammersley, S.O. Svensson, M. Hanfland, A.N. Fitch, D. Häusermann, High Pressure Res. 14 (1996) 235.
[35] S. Vogel, L. Ehm, K. Knorr, G. Braun, Adv. X-ray Anal. 45 (2002) 31.
[36] J. Rodriguez-Carvajal, FULLPROF SUITE, (2003) LLB Sacley & LCSIM Rennes, France.
[37] PCTPro-2000—Calorimetry and thermal analysis, 〈http://www.setaram.com/PCTPro-200.htm〉.
[38] D.R. Lide, CRC Handbook of Chemistry and Physics, 88th ed., CRC, Boca Raton, 2007, pp. 12–27.
[39] Y. Filinchuk, H. Hagemann, Eur. J. Inorg. Chem. (2008) 3127.
[40] P.D. Pathak, N.G. Vasavada, Acta Cryst. A26 (1970) 655.